RESEARCH

Activation of mitogen-activated protein kinase signaling and development of papillary thyroid carcinoma in thyroid-stimulating hormone receptor D633H knockin mice

Markus Eszlinger[1], **Alexandra Stephenson**[2], **Shideh Mirhadi**[3], **Konrad Patyra**[4], **Michael F Moran**[3], **Moosa Khalil**[5], **Jukka Kero**[4,6] and **Ralf Paschke**[1,2,5,7]

[1]Department of Oncology and Arnie Charbonneau Cancer Institute, Cumming School of Medicine, University of Calgary, Heritage Medical Research Building, Calgary, Alberta, Canada, and Institute of Pathology, University Hospital Halle, Halle, Germany
[2]Department of Biochemistry and Molecular Biology, Cumming School of Medicine, University of Calgary, Heritage Medical Research Building, Calgary, Alberta, Canada
[3]Program in Cell Biology, Hospital for Sick Children, and Department of Molecular Genetics, University of Toronto, Peter Gilgan Centre for Research and Learning, Toronto, Ontario, Canada
[4]Research Centre for Integrative Physiology and Pharmacology, Institute of Biomedicine, University of Turku, Turku, Finland
[5]Department of Pathology and Laboratory Medicine, Cumming School of Medicine, University of Calgary, Calgary, Alberta, Canada
[6]Department of Pediatrics, Turku University Hospital, Turku, Finland
[7]Department of Medicine, Cumming School of Medicine, University of Calgary, Heritage Medical Research Building, Calgary, Alberta, Canada

Correspondence should be addressed to R Paschke: ralf.paschke@ucalgary.ca

Abstract

Objective: Nonautoimmune hyperthyroidism (NAH) is rare and occurs due to a constitutively activating thyroid stimulating hormone receptor (TSHR) mutation. In contrast to other thyroid nodules, no further evaluation for malignancy is recommended for hot thyroid nodules. In the first model for NAH in mice nearly all homozygous mice had developed papillary thyroid cancer by 12 months of age.
Methods: To further evaluate these mice, whole exome sequencing and phosphoproteome analysis were employed in a further generation of mice to identify any other mutations potentially responsible and to identify the pathways involved in thyroid carcinoma development.
Results: Only three genes (*Nrg1*, *Rrs1*, *Rasal2*) were mutated in all mice examined, none of which were known primary drivers of papillary thyroid cancer development. Wild-type and homozygous TSHR D633H knockin mice showed distinct phosphoproteome profiles with an enrichment of altered phosphosites found in ERK/mitogen-activated protein kinase (MAPK) signaling. Most importantly, phosphosites with known downstream effects included BRAF p.S766, which forms an inhibitory site: a decrease of phosphorylation at this site suggests an increase in MEK/ERK pathway activation. The decreased phosphorylation at BRAF p.S766 would suggest decreased AMP-activated protein kinase (AMPK) signaling, which is supported by the decreased phosphorylation of STIM1 p.S257, a downstream AMPK target.
Conclusion: The modified phosphoproteome profile of the homozygous mice in combination with human literature suggests a potential signaling pathway from constitutive TSHR signaling and cAMP activation to the activation of ERK/MAPK signaling. This is the first time that a specific mechanism has been identified for a possible involvement of TSH signaling in thyroid carcinoma development.

Keywords

- thyroid
- cancer
- hot thyroid nodules
- mouse model

https://etj.bioscientifica.com
https://doi.org/10.1530/ETJ-23-0049

Introduction

Nonautoimmune hyperthyroidism (NAH) is caused by a constitutively activating thyroid stimulating hormone receptor (TSHR) germline mutation. Germline mutations in TSHR lead to sporadic and familial NAH (SNAH, FNAH) whereas somatic mutations lead to hot thyroid nodules (HTN). Somatic point mutations that constitutively activate the TSHR were first identified in HTN (1). Subsequently, TSHR germline mutations were identified (2). Somatic and germline TSHR mutations show similar gene expression profiles (3). Current evidence suggests that these mutations explain the clinical phenotype of HTN through their activation of the G_s or the G_s and $G_{q/11}$ pathway, resulting in a stimulation of proliferation and differentiation/hormone synthesis (4, 5, 6, 7, 8, 9).

At variance with most other thyroid nodules, current textbooks and guidelines assess HTN as a low cancer risk with no further malignancy evaluation recommended (10). To understand the role of TSHR signaling in the development of hyperthyroidism and thyroid growth, a knockin (KI) mouse model harboring a patient-derived TSHR D633H mutation was generated (11). This mutation has been reported 13 times in hot thyroid adenoma and once in thyroid carcinoma (12). Interestingly, this is one of the few activating mutations with a proposed molecular mechanism of TSHR activation: the disruption of a specific H-bonding network formed between the central regions of transmembrane domain 6 and transmembrane domain 7 which has been proposed as essential for maintaining inactivation of the TSHR (13). For the first time, we found that in the TSHR D633H KI mouse model NAH is not as stable as expected but rather is a dynamic condition involving age, sex, and *Tshr* allele-dependent compensatory mechanisms (11). However, most interestingly, our data strongly suggest that a permanently active TSHR can lead to the malignant transformation of thyrocytes. After 12 months, papillary thyroid carcinoma (PTC) occurred in both heterozygous (HEZ) and homozygous (HOZ) TSHR D633H KI mice with the highest prevalence in HOZ females (11). While the majority of PTCs in humans are typically characterized by a permanently active mitogen-activated protein kinase (MAPK) signaling due to mutations in *BRAF* or one of the *RAS* genes (14, 15), no such mutations were found in the PTCs of TSHR D633H KI animals (11). However, increased ERK1/2 and phospho-ERK1/2 staining was found in the mice harboring PTC (11). Together, this suggests involvement of the TSHR through activation of MAPK, in the development of PTC in this model.

Possible mechanisms for a transition of a subset of thyroid adenomas to thyroid carcinomas have repeatedly been discussed (16, 17, 18, 19). To date, 21 case reports for hot thyroid carcinomas have been published (12) and a recent structured meta-analysis demonstrated an OR of 0.45 for malignancy in HTNs suggesting that while the risk is reduced from that of nontoxic nodules, it is higher than previously believed (20). Moreover, graded TSH suppression according to recurrence risk is the backbone of current thyroid cancer recurrence risk reduction strategies (10). We therefore further investigated the TSHR D633H mutation KI mouse model's genome and phosphoproteome to identify the respective responsible signaling pathway(s) for the evolution of PTCs and the degree to which the TSHR is involved.

The current study provides strong evidence for TSHR's role in PTC development and suggest that TSHR mutations alone may act as a driver mutation in mice. Furthermore, ERK/MAPK signaling was further implicated and a potential pathway from TSHR activation to MAPK signaling is supported by phosphoproteome data.

Materials and methods

TSHR D633H KI mice, animal husbandry, and genotyping

In the preceding study a KI mouse model was generated harboring the TSHR D633H mutation (11). Mice were housed under controlled conditions (IVC units, 12-h light:12-h darkness, 21 ± 1°C) at the Central Animal Laboratory, University of Turku. Animals were provided access to water and pelleted chow *ad libitum* (SDS RM-3 (P); Special Diet Service). The chow contained 0.4 mg/kg iodine, which has been previously shown to be sufficient for thyroid function (21). For hormone analysis, blood from the lateral saphenous vein or via cardiac puncture was collected. Animals were sacrificed with CO_2. For the phenotypic characterization, WT littermates were used as controls.

Morphological characterization and hormone measurements

For ten mice from each group (separated by genotype (HOZ/WT) and sex (M/F)), body weight, body length, tail length, and thyroid weight was recorded at sacrifice. A volume of 0.5–1 mL blood was collected, and the serum was separated for serum TSH and total T4 measurement. Each lobe of the thyroid was preserved separately, one as

https://etj.bioscientifica.com
https://doi.org/10.1530/ETJ-23-0049

formalin-fixed, paraffin-embedded (FFPE) blocks, and one lobe was flash frozen in liquid nitrogen.

Total thyroxine (TT4; #DNOV054) serum concentrations were determined using a commercially available enzyme-linked immunosorbent assay (Novatec). Serum TSH levels were analyzed with the Mouse Pituitary Magnetic Bead Panel (#MPTMAG-49K; Merck Millipore) according to the manufacturer's instructions as previously described (11).

Histology

For nine mice from each group (separated by genotype [HOZ/WT] and sex [M/F]), formalin-fixed (10% formalin in phosphate-buffered saline [PBS]), paraffin-embedded tissue samples were cut using microtome (Leica) into 4 µm sections and stained with hematoxylin and eosin for histological analysis using standard methods. Stained sections were scanned with a Panoramic 250 Flash III Digital Slide Scanner (3D HISTECH). For the classification of thyroid neoplasia, the definition of the World Health Organization on 'Tumours of the Thyroid and Parathyroid' was used (22). Histology was examined by two experienced pathologists (Drs Moosa Khalil and Ronald Ghossein) independently from each other as was described for the previous generation of these mice (11).

Study approval

All experiments were authorized by the National Animal Experiment Board of Finland (License number: 10266).

Statistical analysis

GraphPad Prism v7 (GraphPad Software, Inc.) was used for statistical analysis. An unpaired t-test and one-way analysis of variance with Dunnett's *post hoc* test and nonparametric Kruskal–Wallis test were used to determine statistical significances. A *P*-value of <0.05 was set as the limit of statistical significance.

Whole exome sequencing (WES)

Input samples (DNA isolated from thyroid tissue) were normalized to 100 ng and sheared by Covaris to 200 bp. Libraries were prepared using the Agilent SureSelect XT HS Target Enrichment Kit for Illumina, captured in single plex with baits from the Agilent SureSelect XT CD Mouse All Exon V2 kit. The libraries were pooled and sequenced on an Illumina NovaSeq6000 SP flowcell in 2 × 100 cycle configuration using NEB Unique Dual Indices. Small nucleotide variants were called using Illumina Dragen version 07.021.510.3.5.7 using the standard variant caller pipeline against reference genome mm10. Genomic alterations of interest met the following criterion: variants found in DNA from more than one TSHR D633H KI HOZ mouse in >10 reads.

Phosphoproteome analysis

Preparation of phosphopeptide eluates and analysis by liquid chromatography tandem mass spectrometry (LC-MS/MS) using an EASY-nanoLC 1200 system and an Orbitrap Fusion™ Lumos™ Tribrid™ Mass Spectrometer (Thermo Fisher Scientific) is described in Supplementary Methods File 1 (see the section on Supplementary Materials given at the end of this article).

Phosphoproteome normalization

Normalization was performed by using the control bridges per peptide by internal reference scaling (23). Normalization was successful as evidenced by absence of clustering by isobaric label group or TMT experimental group clustering.

Statistical analyses of phosphoproteome data

Phosphoproteome hierarchical clustering and principal component analysis (PCA) were performed on the subset of peptides quantified in all samples by Spearman's rho clustering method for both rows and columns.

Phosphoproteome intensities are log2 transformed and z-score across respective samples. For sample (columnwise) and protein (rowwise) clustering, Spearman's rho correlation distance with average linkage was used using Perseus software default parameters. Volcano analysis was performed, where all phosphopeptides detected in at least 70% of samples was compared between the two groups with 0.05 false discovery rate and s0 = 0.1 parameter.

Results

Female TSHR D633H KI mice have lower TSH and higher thyroid weight and exhibit increased PTC prevalence at 12 months of age

Similarly to the previous description (11), the TSH is significantly lower in HOZ TSHR D633H KI males

https://etj.bioscientifica.com
https://doi.org/10.1530/ETJ-23-0049

(P < 0.01) and females (P < 0.001) than their WT littermates (Supplementary Fig. 1A and E). There is no significant difference between total T4 in HOZ and WT in either sex (Supplementary Fig. 1B and F). Body weight is significantly lower in HOZ female mice than WT (P < 0.01) (Supplementary Fig. 1C and G). Thyroid weight is significantly higher in both HOZ males (P < 0.001) and females (P < 0.001) compared to WT (Supplementary Fig. 1D and H). In nine thyroids from HOZ females for which slides from throughout FFPE block were reviewed, eight were positive for PTC (88%); in nine male HOZ samples for which the slides from throughout the FFPE block were reviewed, five were positive for PTC (55%) (Supplementary Fig. 2).

WES uncovers no further causative mutations

WES was performed on one lobe of five female HOZ mice and three female WT mice, respectively. All five HOZ mice had confirmed PTC in the contralateral FFPE preserved lobe. In a first filtering step, the sequence variants identified in the HOZ mice were compared against the sequence variants detected in the WT mice and overlapping variants were excluded. In a second filtering step, the HOZ mice specific variants were filtered to exclude intronic variants, silent variants, ncRNAs and variants with less than ten variant reads resulting in 330 remaining variants. 13 variants were found in more than one mouse (Fig. 1). First, the introduced *TSHR* mutation p.D633H could be detected in all five analyzed mouse samples. In addition, the *Nacad* frameshift mutation p.P37fs, the *Nrg* variant p.T463N and four different *Rrs1* variants were also detected in the five analyzed mouse samples (Table 1, Fig. 1). Furthermore, in four out of five mice the *Rasal2* variant p.E453K was detected. While in three out of five mice samples variants were detected in *Kpna4*, *Narf* and *Net1*, variants in *Ddias*, *Thap1*, *Ankrd36*, *Pgk2*, and *Pou3f3* were detected in two mice each.

The involvement of the 13 mutated genes in carcinogenesis was evaluated using COSMIC database for humans, and candidate cancer gene database (CCGD) for mice (Table 1) (24, 25). According to CCGD, for none of the mutant genes a mouse model could be identified that would support a role in thyroid cancer (Table 1). Furthermore, using the COSMIC database we identified the percentage of human thyroid samples with detected variants in the genes identified by WES in our mice. The highest prevalence in thyroid samples was reported for *TSHR*

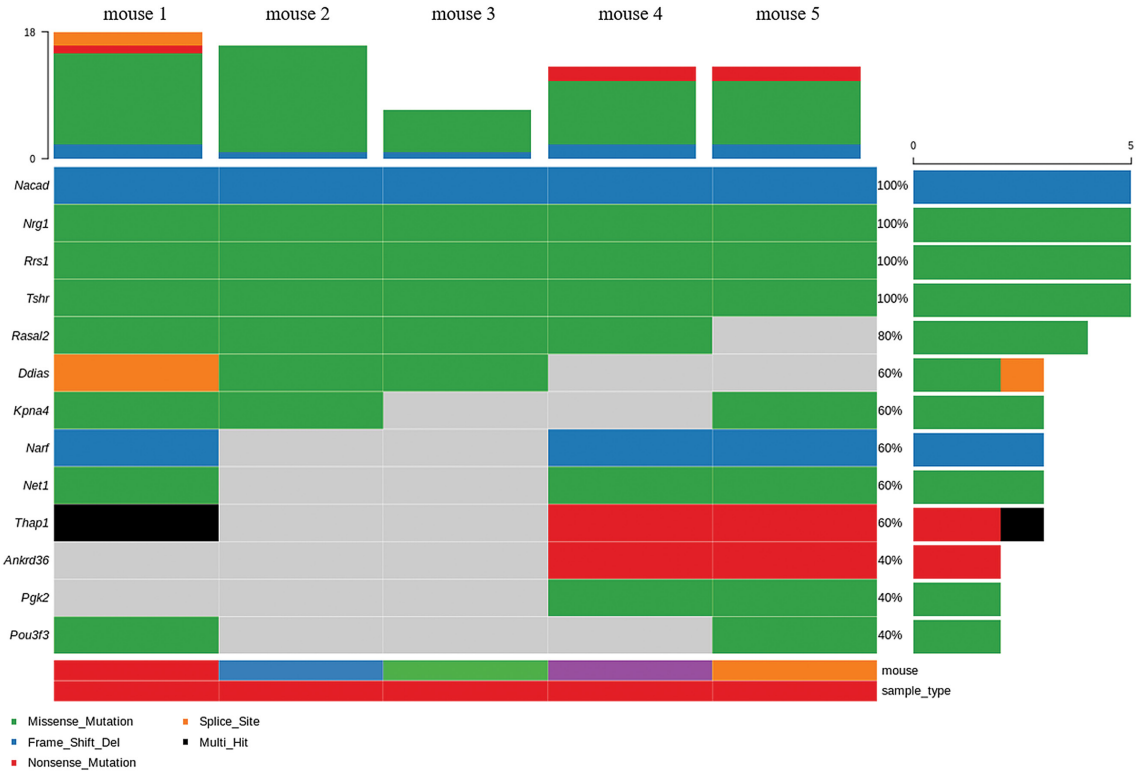

Figure 1
Genes in which the top most prevalent variants were found by WES of five homozygous female mice in >10 reads

https://etj.bioscientifica.com
https://doi.org/10.1530/ETJ-23-0049

Table 1 Genes with mutations found in DNA from more than one TSHR D633H KI HOZ mouse with >10 variant reads. CCGD ranking of evidence from A–D based on point mutation and copy number variation. The relative rank is unique to each study and cannot be used to compare across all results (24).

		Mice samples			Human thyroid samples‡	
Gene	Gene name	M/T†	Mutations detected	CCGD evidence*	M/T†	%
Nacad	NAC Alpha Domain Containing	5/5	P37fs	Liver (D), Colorectal (N/A)	42/1040	4%
Nrg1	Neuregulin 1	5/5	T463N	N/D	4/1040	0.4%
Rrs1	Ribosome Biogenesis Regulator 1 Homolog	5/5	G54V (3), R44H (2), R51C (2), V49M (2)	N/D	9/1040	0.9%
Tshr	Thyroid Stimulating Hormone Receptor	5/5	D633H	N/D	350/3338	10.5%
Rasal2	RAS Protein Activator Like 2	4/5	E453K	Nervous System (C)	10/1040	1%
Kpna4	Karyopherin Subunit Alpha 4	3/5	V280I	Liver (A,A,D), Blood (B,C), Colorectal (A,B,C,C,C), Pancreatic (C), Gastric (B), Nervous System (C)	11/1040	1.1%
Narf	Nuclear Prelamin A Recognition Factor	3/5	A319fs	Blood (B)	15/1040	1.4%
Net1	Neuroepithelial Cell Transforming 1	3/5	A444V	Liver (D,D)	12/1040	1.2%
Ddias	DNA damage-induced apoptosis suppressor	2/5	P706L	N/D	3/1040	0.3%
Thap1	THAP Domain Containing 1	2/5	K89_K90delinsKKEDLES QEQLPSASPPCFPGX	N/D	0/1040	0%
Ankrd36	Ankyrin Repeat Domain 36	2/5	Y89_D90delinsX	Blood (D)	77/1040	7.4%
Pgk2	Phosphoglycerate Kinase 2	2/5	G213S	N/D	2/1040	0.2%
Pou3f3		2/5	M370T	N/D	11/1040	1.1%

†Mutations in respective gene; *CCGD database evidence of cancer-causing role in mice (relative rank within study); ‡COSMIC database v95.
M/T, mutated/tested; N/A: not available, N/D: not detected.

mutations (10.5%), followed by *Ankrd36* and *Nacad* variants found in 7% and 4%, respectively (25). All remaining mutated genes identified by WES in our mice were found mutated in approximately 1% or less of the COSMIC human thyroid samples (Table 1).

TSHR HOZ thyroids have distinct phosphoproteome profiles

Phosphoproteome profiling was performed for 18 HOZ mice (eight females, ten males) and 18 WT mice (eight females, ten males), respectively. Of the 3900 phosphopeptides quantified, majority were serine (S) followed by threonine (T) and finally tyrosine (Y) residues (Fig. 2A). Based on an unbiased hierarchical Spearman's rho clustering of phosphopeptides, two major clusters are formed. One with 17 WT and one HOZ mouse, the other including 17 HOZ and one WT mouse (Fig. 2B). Of the 36 samples analyzed, all but two male samples (one WT and one HOZ) clustered within their genotype (Fig. 2B). Applying a PCA including both genotype and sex confirms the findings of the hierarchical clustering demonstrating a very clear separation of mice into WT and HOZ clusters (Fig. 2C). Moreover, among HOZ samples a clear distinction between sex is also seen, but it is noticeable that the male HOZ mice show significantly weaker differences compared to the WT mice than the female HOZ mice (Fig. 2B and C). This can be due to baseline differences that exist between males and females for TSH pathway.

To identify these baseline sex differences, the phosphorylation patterns of phosphopeptides of WT males and females were compared to one another. Significantly different phosphorylation patterns between male and female mice could be identified for 142 phosphopeptides (Supplementary Table 1). Phosphorylation of thyroglobulin was significantly lower in WT males compared to WT females but at a similar level as the HOZ mice of both sexes (Fig. 2D). The same analysis was completed for HOZ mice without any significantly different phosphosites identified.

Pathway enrichment analysis emphasizes changes in MEK/ERK signaling

148 significantly differential phosphosites between all WT and HOZ samples were identified using volcano analysis (Fig. 3A). Based on those phosphosites a list of significantly enriched pathways was generated using Ingenuity Pathway Analysis tool (Qiagen) (Fig. 3B). The same analyses were performed sex-specifically for females only

https://etj.bioscientifica.com
https://doi.org/10.1530/ETJ-23-0049

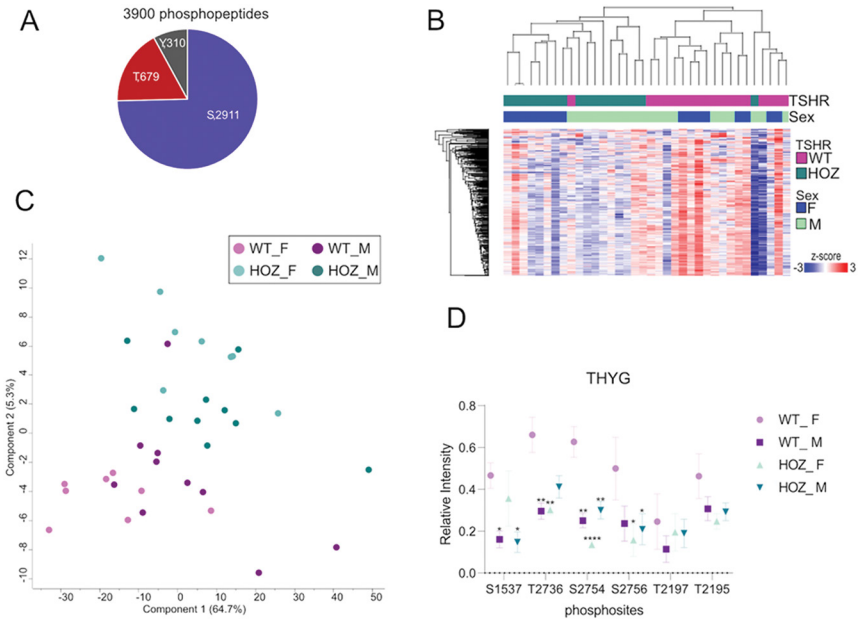

Figure 2
Clustering and Separation of samples. (A) Composition of quantified phosphopeptides. (B) Unbiased hierarchical Spearman's rho clustering of phosphopeptides found in all samples forms two major clusters with one composed of mostly wild-type (WT) samples and the other mostly composed of homozygous (HOZ) samples. In cluster composed of HOZ but not WT, samples further cluster based on sex. (C) Principal component analysis (PCA, c1 × c3) showing separation of samples by TSHR and sex. (D) Relative intensities of thyroglobulin phosphosites

identifying 268 significantly differential phosphosites between WT and HOZ samples (Fig. 3C and D) and males only identifying one significant differential phosphosite (CLIP4) between WT and HOZ samples (Supplementary Fig. 3), respectively.

The following pathways of interest based on their known association with thyroid or thyroid cancer signaling were selected from the list of significantly enriched pathways: ERK/MAPK signaling, protein kinase A signaling, insulin receptor signaling, Rho family GTPases, and molecular mechanisms of cancer. The signaling pathways were overlaid with phosphosites significantly enriched in female HOZ mice (Fig. 4, Supplementary Figs. 4, 5, 6, and 7). The known upstream and downstream effects of these phosphosites were summarized for ERK/MAPK signaling (Table 2). Most importantly, phosphosites with known downstream effects included BRAF p.S766 (Fig. 5).

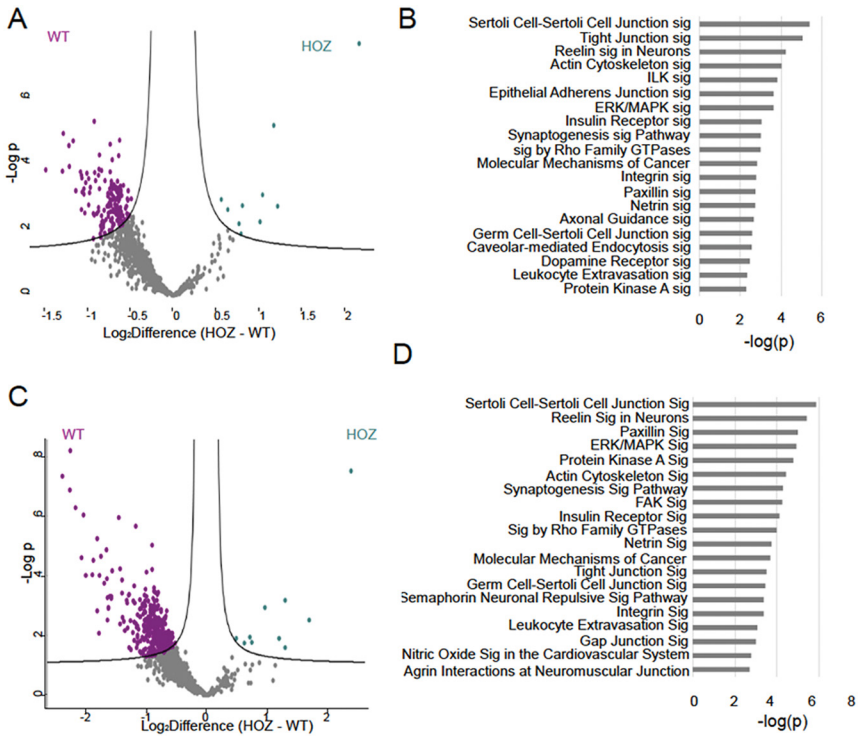

Figure 3
Differential phosphosites between wildtype (WT) and homozygous (HOZ) samples. (A) Volcano plot on phosphopeptides found in at least 70% of all samples comparing HOZ to WT (FDR < 0.05). (B) Top significant enriched pathways by ingenuity pathway analysis. (C) Volcano plot on phosphopeptides found in at least 70% of female samples comparing HOZ to WT (FDR < 0.05). (D) Top significant enriched pathways ingenuity pathway analysis in female mice.

https://etj.bioscientifica.com
https://doi.org/10.1530/ETJ-23-0049

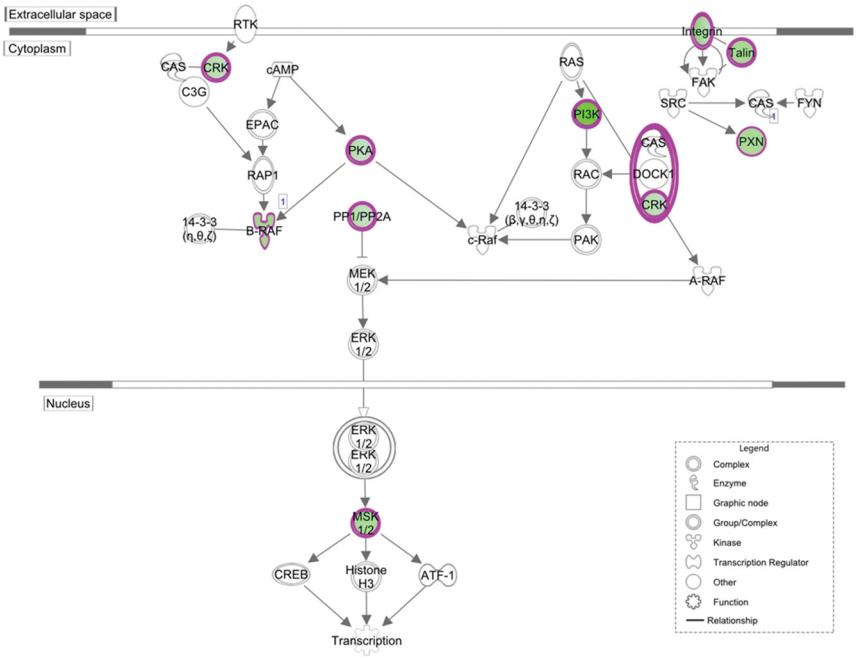

Figure 4
Simplified ERK/MAPK signaling pathway overlaid with phosphosites significantly enriched in homozygous (HOZ) vs wild type (WT).

Discussion

We have shown that the majority of mice with constitutive TSHR mutation p.D633H develop PTC. While the molecular etiology for human PTC is well understood, in our model no mutations in the known causative genes were detected. Phosphoproteome analysis demonstrated a clear separation based on differentially phosphorylated proteins between female WT and HOZ mice. While an unbiased pathway analysis found several significantly enriched pathways, the increased ERK/MAPK signaling in HOZ female mice is in line with previous findings (11) and clearly demonstrates a potential link between TSHR and MAPK signaling.

Female TSHR D633H KI mice have a more severe hyperthyroidism and carcinoma phenotype

In this generation of mice, HOZ mice of both sexes demonstrate subclinical hyperthyroidism: decreased TSH without accompanying increased T4 (Supplementary Fig. 1) in contrast to the previous generation's overt hyperthyroidism in females (11). The comparison of TSH levels between male and female mice revealed higher TSH levels in male mice, which is comparable to the previous generation of mice (11). In contrast, male and female mice are characterized by comparable total T4 levels, which are slightly higher compared to the previous generation of mice (with exception of the female HOZ mice) (11).

Table 2 ERK/MAPK pathway enriched phosphopeptides in homozygous mice and their known upstream/downstream effectors.

Symbol	Entrez gene name	Phosphosite	Upstream	Downstream
BRAF	B-Raf proto-oncogene, serine–threonine kinase	S766	AMPKA1	Cell growth inhibited
CRK	CRK proto-oncoqene, adaptor protein	S43	Uncharacterized	Uncharacterized
CRKL	CRK-like proto-oncogene, adaptor protein	S107	Uncharacterized	Uncharacterized
ITGA1	Integrin subunit alpha 1	Y715	Unknown	Unknown
PIK3R4	Phosphoinositide-3-kinase regulatory subunit 4	S18	Unknown	Unknown
PPP1R7	Protein phosphatase 1 regulatory subunit 7	S24	PLK1	
PPP1R14A	Protein phosphatase 1 regulatory inhibitor subunit 14A	S134	Uncharacterized	Uncharacterized
PRKAR1A	Protein kinase cAMP-dependent type I regulatory subunit alpha	S77	Metastatic potential	Molecular association regulation
PRKAR2A	Protein kinase cAMP-dependent type II regulatory subunit alpha	T101	Uncharacterized	Uncharacterized
PXN	Paxilin	S321	Uncharacterized	Uncharacterized
RPS6KA4	Ribosomal protein S6 kinase A4	S681	Uncharacterized	Uncharacterized
TLN1	Talin 1	S1328	Uncharacterized	Uncharacterized

https://etj.bioscientifica.com
https://doi.org/10.1530/ETJ-23-0049

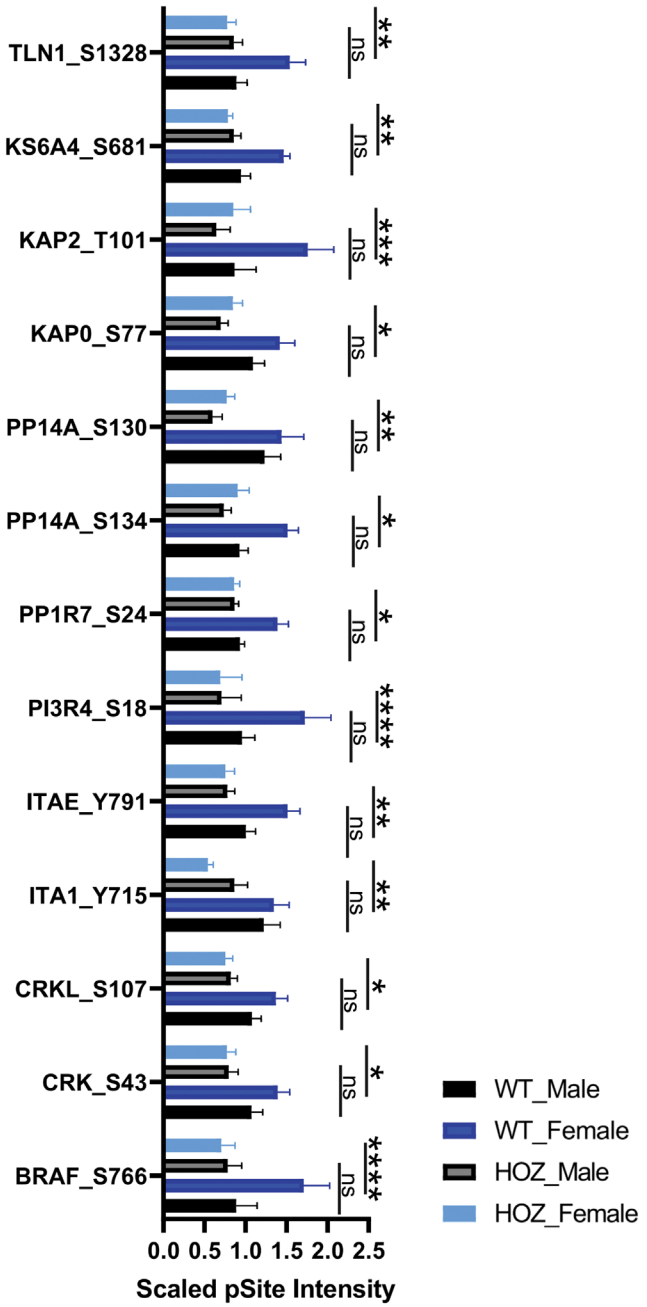

Figure 5
ERK/MAPK pathway-enriched phosphopeptides. pY sites are plotted for WT and HOZ female and male mice (mean ± S.E.M.). *P*-values determined by two-way ANOVA multiple comparison and plotted for male WT vs HOZ and female WT vs HOZ comparison (*$P < 0.05$, **$P < 0.005$, ***$P < 0.0005$, ****$P < 0.00005$).

TSH differences among sexes have been reported in mice but with high variability depending on the mice strain. Therefore, one could speculate that a particular mice strain background could be a possible reason for the higher percentage of PTCs in females (88% vs 55% in males), which was also observed in the previous generation (females 88% vs males 71%). However, also in humans, hyperthyroidism and thyroid cancer occur about three times more often in women than in men.

The decreased body weight in females may reflect a more severe hyperthyroid phenotype, consistent with the previously described generation (Supplementary Fig. 1C and G) (11). The higher PTC incidence in females (Fig. 2) is consistent with the increased degree of affectedness of females in this model that was previously observed and also fits with the fact that both benign and malignant thyroid disorders affect women three to four times more than men (11, 26, 27, 28). The baseline differences in phosphorylation observed in the WT mice, namely, the lower baseline phosphorylated thyroglobulin levels in males, could explain the differences seen in this model. Sex differences in thyroglobulin serum concentrations are not observed in humans (29, 30).

TSHR variant as a driver mutation for thyroid carcinoma

Whole-exome sequencing (WES) was performed on female mice based on the higher frequency of PTC in female mice and the subjective observation that PTCs in female mice were larger and constituted more of the thyroid. Based on the morphological data indicating a relatively consistent phenotype among TSHR D633H KI HOZ mice, our focus for WES data analysis was on genes mutated in more than one mouse (Table 1). Using the COSMIC database, we assessed the prevalence of the variants detected by WES in 1040 human thyroid carcinomas. In addition, a CCGD search was done to rule out a variant that is mouse-specific in inducing thyroid cancer (24, 25). There were no published mice data suggesting involvement of any of the top twenty genes in thyroid carcinoma according to CCGD nor were any of these genes mutated in more than 15% of thyroid cancer samples in the COSMIC database. A literature search for cases of thyroid carcinoma with these variants was performed to better understand their role in carcinogenesis.

Nacad, Nrg1 and Rrs1 were mutated in all five HOZ samples submitted for WES (Fig. 1) and had a respective variant prevalence in human thyroid cancer of 4%, 0.4% and 0.9% according to the COSMIC database, respectively. Since all variants detected in HOZ mice were filtered for variants detected in a pool of three WT mice, a mice strain specific occurrence of the identified variants can be excluded. In contrast, variants detected in all five HOZ mice could be the result of a common second hit mechanism induced by hyperproliferation of thyrocytes

https://etj.bioscientifica.com
https://doi.org/10.1530/ETJ-23-0049

in the HOZ mice. *Nrg1* is an epidermal growth factor-like family member with many roles including cell signaling mediation and organ growth and development. While the p.T463N *Nrg1* variant detected in this mouse model has not previously been described, increased NRG1 expression in humans showed moderate association with a more aggressive course of BRAF mutation positive PTCs (31, 32).

In humans, *RRS1* gene expression is significantly increased in thyroid carcinoma compared to paired pericarcinous tissues and PTC cells in culture showed reduced cell proliferation, cell cycle and increased apoptosis when *RRS1* was knocked out (33).

Limited data exist for *Nacad*, however, as it is known to be primarily expressed in the brain, followed by the ovaries, adrenal glands and testis, with very low expression in the thyroid it's involvement in the carcinoma phenotype is unlikely (34).

Rasal2, the inhibitory regulator of the Ras cAMP pathway with a known role in breast and lung cancer (35, 36), *Ddias,* a DNA damage induced apoptosis suppresser which is upregulated by ERK signaling (37), *Kpna4* an oncogene with a role in PTC cell proliferation and invasion shown to be overexpressed in PTC cells (38), and *Thap1*, also shown to be overexpressed in PTC cells may all have a role in PTC development. However, variants in these genes were found only in a subset of mice. As the phenotype across all five female mice is consistent, this suggests that none of these genes are primarily responsible for the carcinoma in our model, although likely may play secondary roles in some mice as described above for *Nrg1* and *Rrs1*.

For the remaining genes mutated in less than 5 mice there is no evidence in the literature for a role in thyroid carcinoma.

Based on our analysis, there are thus no obvious primary causative mutations in addition to the TSHR mutation in these TSHR D633H KI mice. While a potential secondary role in the development of PTC for one or more of these additional variants detected by WES, particularly Nrg1 and Rrs1 could be possible, there is no obvious candidate for a primary driver mutation other than the TSHR mutation.

In humans, *TSHR* mutations were found in 2% of COSMIC database thyroid carcinoma samples (Database accessed February 11 2022; search query *TSHR*). While this is a low number, the prevalence of hot thyroid carcinomas is equally low. As of 2020, there were 21 published cases of human thyroid carcinoma with *TSHR* mutations. Of these 21 cases, three reported further mutations (1 *KRAS*, 1 *NRAS* and 1 *PAX8-PPARG*), seven have reported negative results for analysis of additional mutations, although the further genes assessed vary. Histologic diagnoses were 13 FTC, six PTC, one Hurthle cell thyroid cancer, and one insular thyroid cancer ((12), https://tsh-receptor-mutation-database.org). Also, *TSHR* mutations have been suggested to be associated with an increased cancer risk (39). Taken together, the WES results of the mice thyroids without a detection of a likely driver mutation in addition to the introduced *TSHR* mutation, and the molecular data reported for hot thyroid carcinomas in humans support the hypothesis that the mechanism of PTC formation in our mouse model is likely novel and caused by *TSHR* mutation.

Sex differences

The reasons for the 3-4fold increased rates of benign and malignant thyroid disorders in women is not well understood (11, 26, 27, 28). In an attempt to unravel some of the differences in signaling, phosphorylation profiles were compared across sexes in WT and in HOZ mice. Interestingly, WT males showed a lower thyroglobulin phosphorylation compared to WT females but at a similar level as the HOZ mice of both sexes. In fact, comparing male HOZ and WT mice revealed only one significantly different phosphopeptide (CLIP4) based on *t*-test FDR <0.05. CLIP4 showed the same phosphorylation pattern when comparing female HOZ and WT mice. CLIP4 is located in an intracellular membrane-bounded organelle and is predicted to be involved in cytoplasmic microtubule organization. More research is needed to elucidate the reasons for sex differences in this model and in human thyroid disorders.

The connection between TSHR and MAPK signaling

Many cancers have associated dysregulated kinase signaling whether this is through kinase overexpression, mutations in kinase genes, or defects in counterregulatory mechanisms (40, 41). While genomic changes such as a *TSHR* mutation in a carcinoma without any other driver mutations are the first step to understanding the mechanism of carcinogenesis, it is essential to understand the consequences in signaling in order for this information to inform the etiology of thyroid cancer in general. For this reason, following our WES result, phosphoproteome analysis was performed.

TSHR signaling via cAMP is increased by the D633H KI mutation, as evidenced by the 5.4-fold increase in basal cAMP signaling for the TSHR (11, 13, 42). Furthermore,

https://etj.bioscientifica.com
https://doi.org/10.1530/ETJ-23-0049

cAMP signaling has been shown to activate MAPK signaling (43, 44). Within the BRAF protein, a central component of the MAPK pathway, serine-729 (p.S729) forms an inhibitory site: when phosphorylation at this site occurs by AMPK, it has been shown to inhibit the phosphorylation/activation of downstream MEK/ERK (45, 46). Vice versa, a decrease of phosphorylation at this site suggests an increase in MEK/ERK pathway activation. Interestingly, the homologous position of the human BRAF p.S729 in mice, Braf p.S766, is characterized by decreased phosphorylation in HOZ mice (Table 2, Fig. 5). While further downstream ERK/MEK phosphopeptides were not identified or quantified by this analysis, phosphorylated ERK1/2 characterized by immunohistochemistry was seen in the carcinoma lesions of this model (11). The decreased phosphorylation at Braf p.S766 in HOZ females would suggest decreased AMPK signaling which is supported by the decreased phosphorylation of STIM1 p.S257, a downstream target of AMPK (47). Furthermore, AMPK inactivation downstream of TSHR has been suggested multiple times (48, 49, 50, 51, 52) and evidence of AMPK inhibition by cAMP signaling (53) offers a direct mechanism for the signaling changes found in this model (Fig. 6).

Further supporting the role of aberrant cAMP signaling is differential Prkar1a phosphorylation at p.S77 (Table 2, Fig. 5). This is a regulatory subunit of protein kinase A (PKA), responsible for regulating activity downstream of PKA in response to cAMP. While the downstream effects of phosphorylation at this site are not known, alterations in PKA activity can lead to numerous different effects based on a variety of factors including cAMP basal levels which are higher than WT in this model (11, 54). Upstream metastatic potential has also been observed (55). In humans, *PRKAR1A* mutations are found in more than half of patients with Carney Complex (CNC) (56). This condition results in increased cAMP signaling and also demonstrates rare PTCs in addition to benign HTN (57). Based on these findings we propose a signaling pathway for the development of thyroid cancer in our mouse model as summarized in Fig. 6.

In our previous study (11) we speculated that the simultaneous activation of Gq/11, in addition to Gs could be an important player in tumor formation in the TSHR D633H KI mouse model because α1B-adrenergic receptor mutant mice show malignant transformation of thyrocytes along with activation of both Gs and Gq/11 signaling pathways (58). Nevertheless, by immunohistochemistry, we also saw an increased phosphorylation of ERK1/2 in the PTC areas of the TSHR D633H KI mice (11), which argues for an activation of the MAPK signaling pathway. Indeed, TSH signaling can converge toward a MAPK growth signal, for example via Gs, EPAC and/or RAP1B as shown previously in thyrocyte models (43, 44). Despite in a different way, the current findings support the latter, a link between Gs signaling and MAPK activation. Overall, based on the previous data showing potential relevance of Gq/11 signaling (for which we found no evidence at the phosphoproteome level) and on our previous and current data showing a specific phosphorylation pattern supporting a Gs - MAPK link, we can speculate that both arms of TSHR signaling, via Gs and Gq/11, are important for the malignant transformation in the PTC areas seen in our mouse model.

We acknowledge that in addition to our descriptive phosphoproteome analyses further functional studies are needed to precisely elaborate the mechanism behind the molecular patterns we have observed in this study.

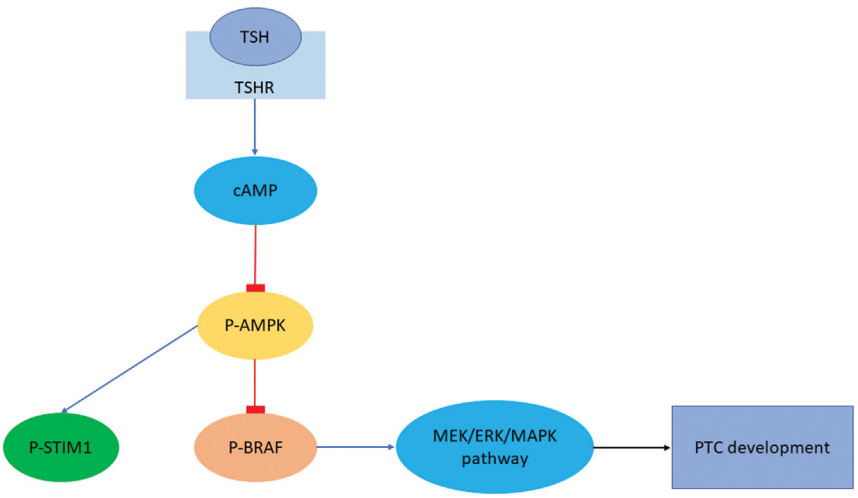

Figure 6
Proposed signaling pathway leading to increased MEK/ERK signaling in TSHR D633H KI mouse model.

https://etj.bioscientifica.com
https://doi.org/10.1530/ETJ-23-0049

It would be interesting to investigate if the effects on AMPK/BRAF/MEK/ERK pathway are directly caused by TSHR hyperactivation through cAMP or if the metabolic alterations induced by the hyperthyroid state could play a role as well, since many different signaling pathways influenced by metabolic changes can modulate AMPK activity and signaling.

It is not the first time TSHR signaling has been implicated in thyroid cancer. TSHR signaling has been suggested to have a role in a genetic predisposition to PTC (59). High-normal serum TSH is associated with a higher risk for differentiated thyroid cancer in thyroid nodule patients (60) and thyroid cancer in patients with thyroid nodules is predicted by baseline serum TSH concentrations (61). Furthermore, there are 21 published cases of *TSHR* mutation positive hot thyroid carcinomas (12) and TSHR signaling is implicated in the development of thyroid carcinoma as well as severity of thyroid carcinoma phenotype (62, 63, 64). Finally, our mouse data demonstrate a signaling pathway through which Tshr signaling in mice could lead to malignancy via activation of the MAPK pathway downstream of cAMP. In summary, these data impressively demonstrate a key role of the TSHR-cAMP pathway in Braf-induced PTC initiation in mice, and are consistent with the association of TSH levels with thyroid cancer incidence in humans (61).

Conclusions

TSHR D633H KI mice develop PTC while maintaining a subclinical hyperthyroidism phenotype. While the molecular etiology for PTC in humans is generally considered to be well understood, no mutation in known driver genes were detected in the mouse PTCs. Nevertheless, variants that may contribute to a multi-hit model together with the TSHR mutation were identified by WES. Most importantly, phosphoproteome analysis revealed a potential link between Tshr signaling and the MAPK pathway in mice. We identified decreased phosphorylation of Braf p.S766 as the likely specific link by which activation of the cAMP pathway in TSHR D633H mutation KI mice leads to increased MEK/ERK signaling and hence a high incidence of PTCs.

Supplementary materials
This is linked to the online version of the paper at https://doi.org/10.1530/ETJ-23-0049.

Declaration of interest
ME reports: no conflict of interest; AS reports: no conflict of interest; SM reports: no conflict of interest; KP reports: no conflict of interest; MM reports: no conflict of interest; MK reports: no conflict of interest; JK reports: no conflict of interest; RP reports: advisory board honoraria from Bayer and Eisai.; Funding statement.

Funding
The study was funded by a Laura Linders Grant.

Author contribution statement
ME: conceptualization, formal analysis, writing – original draft, writing – review & editing; AS: investigation, formal analysis, writing – original draft; SM: methodology, investigation, formal analysis, KP: investigation; MM: methodology, supervision; MK: investigation; JK: resources, supervision; RP: conceptualization, resources, supervision, writing – review & editing.

Acknowledgements
We thank Ronald Ghossein for his evaluation of the PTC samples.

References

1 Parma J, Duprez L, Van Sande J, Hermans J, Rocmans P, Van Vliet G, Costagliola S, Rodien P, Dumont JE & Vassart G. Diversity and prevalence of somatic mutations in the thyrotropin receptor and Gsα genes as a cause of toxic thyroid adenomas. *Journal of Clinical Endocrinology and Metabolism* 1997 **82** 2695–2701. (https://doi.org/10.1210/jcem.82.8.4144)
2 Duprez L, Parma J, Van Sande J, Allgeier A, Leclère J, Schvartz C, Delisle MJ, Decoulx M, Orgiazzi J & Dumont J. Germline mutations in the thyrotropin receptor gene cause non–autoimmune autosomal dominant hyperthyroidism. *Nature Genetics* 1994 **7** 396–401. (https://doi.org/10.1038/ng0794-396)
3 Hebrant A, Van Sande J, Roger PP, Patey M, Klein M, Bournaud C, Savagner F, Leclere J, Dumont JE, van Staveren WC, *et al.* Thyroid gene expression in familial nonautoimmune hyperthyroidism shows common characteristics with hyperfunctioning autonomous adenomas. *Journal of Clinical Endocrinology and Metabolism* 2009 **94** 2602–2609. (https://doi.org/10.1210/jc.2008-2191)
4 Lüblinghoff J, Nebel IT, Huth S, Jäschke H, Schaarschmidt J, Eszlinger M & Paschke R. The leipzig thyrotropin receptor mutation database: update 2012. *European Thyroid Journal* 2012 **1** 209–210. (https://doi.org/10.1159/000342918)
5 Ferraz C & Paschke R. Inheritable and sporadic non-autoimmune hyperthyroidism. *Best Practice and Research. Clinical Endocrinology and Metabolism* 2017 **31** 265–275. (https://doi.org/10.1016/j.beem.2017.04.005)
6 Vassart G & Dumont JE. The thyrotropin receptor and the regulation of thyrocyte function and growth. *Endocrine Reviews* 1992 **13** 596–611. (https://doi.org/10.1210/edrv-13-3-596)
7 Postiglione MP, Parlato R, Rodriguez-Mallon A, Rosica A, Mithbaokar P, Maresca M, Marians RC, Davies TF, Zannini MS, De Felice M, *et al.* Role of the thyroid-stimulating hormone receptor signaling in development and differentiation of the thyroid gland. *PNAS* 2002 **99** 15462–15467. (https://doi.org/10.1073/pnas.242328999)

8 Stephenson A, Eszlinger M, Stewardson P, McIntyre JB, Boesenberg E, Bircan R, Sancak S, Gozu HI, Ghaznavi S, Krohn K, *et al.* Sensitive sequencing analysis suggests thyrotropin receptor and guanine nucleotide-binding protein G subunit alpha as sole driver mutations in hot thyroid nodules. *Thyroid* 2020 **30** 1482–1489. (https://doi.org/10.1089/thy.2019.0648)

9 Paschke R & Ludgate M. The thyrotropin receptor in thyroid diseases. *New England Journal of Medicine* 1997 **337** 1675–1681. (https://doi.org/10.1056/NEJM199712043372307)

10 Haugen BR, Alexander EK, Bible KC, Doherty GM, Mandel SJ, Nikiforov YE, Pacini F, Randolph GW, Sawka AM, Schlumberger M, *et al.* 2015 American Thyroid Association management guidelines for adult patients with thyroid nodules and differentiated thyroid cancer: the American Thyroid Association guidelines task force on thyroid nodules and differentiated thyroid cancer. *Thyroid* 2016 **26** 1–133. (https://doi.org/10.1089/thy.2015.0020)

11 Jaeschke H, Undeutsch H, Patyra K, Löf C, Eszlinger M, Khalil M, Jännäri M, Makkonen K, Toppari J, Zhang FP, *et al.* Hyperthyroidism and papillary thyroid carcinoma in thyrotropin receptor D633H mutant mice. *Thyroid* 2018 **28** 1372–1386. (https://doi.org/10.1089/thy.2018.0041)

12 Stephenson A, Lau L, Eszlinger M & Paschke R. The thyrotropin receptor mutation database update. *Thyroid* 2020 **30** 931–935. (https://doi.org/10.1089/thy.2019.0807)

13 Neumann S, Krause G, Chey S & Paschke R. A free carboxylate oxygen in the side chain of position 674 in transmembrane domain 7 is necessary for TSH receptor activation. *Molecular Endocrinology* 2001 **15** 1294–1305. (https://doi.org/10.1210/mend.15.8.0672)

14 Network CGAR. Integrated genomic characterization of papillary thyroid carcinoma. *Cell* 2014 **159** 676–690. (https://doi.org/10.1016/j.cell.2014.09.050)

15 Roger PP, van Staveren WC, Coulonval K, Dumont JE & Maenhaut C. Signal transduction in the human thyrocyte and its perversion in thyroid tumors. *Molecular and Cellular Endocrinology* 2010 **321** 3–19. (https://doi.org/10.1016/j.mce.2009.11.015)

16 Montemayor-Garcia C, Hardin H, Guo Z, Larrain C, Buehler D, Asioli S, Chen H & Lloyd RV. The role of epithelial mesenchymal transition markers in thyroid carcinoma progression. *Endocrine Pathology* 2013 **24** 206–212. (https://doi.org/10.1007/s12022-013-9272-9)

17 Dom G, Frank S, Floor S, Kehagias P, Libert F, Hoang C, Andry G, Spinette A, Craciun L & de Saint Aubin N. Thyroid follicular adenomas and carcinomas: molecular profiling provides evidence for a continuous evolution. *Oncotarget* **2018** 10343–10359. (https://doi.org/10.18632/oncotarget.23130)

18 Umbricht CB, Saji M, Westra WH, Udelsman R, Zeiger MA & Sukumar S. Telomerase activity: a marker to distinguish follicular thyroid adenoma from carcinoma. *Cancer Research* 1997 **57** 2144–2147.

19 Takenaka Y, Inohara H, Yoshii T, Oshima K, Nakahara S, Akahani S, Honjo Y, Yamamoto Y, Raz A & Kubo T. Malignant transformation of thyroid follicular cells by galectin-3. *Cancer Letters* 2003 **195** 111–119. (https://doi.org/10.1016/s0304-3835(03)00056-9)

20 FA LL, Robertson H, Stephenson A, Rabi DM & Paschke R. Malignancy risk of hyperfunctioning thyroid nodules compared with non-toxic thyroid nodules: systematic review and meta analysis. *Thyroid Research* 2019 **29**. (https://doi.org/10.1186/s13044-021-00094-1)

21 Maier J, Van Steeg H, Van Oostrom C, Paschke R, Weiss RE & Krohn K. Iodine deficiency activates antioxidant genes and causes DNA damage in the thyroid gland of rats and mice. *Biochimica et Biophysica Acta* 2007 **1773** 990–999. (https://doi.org/10.1016/j.bbamcr.2007.03.011)

22 DeLellis R. Tumors of the thyroid and parathyroid. In *World Health Organization Classification of Tumors*. Lyon: World Health Organization 2004 49–134.

23 Plubell DL, Wilmarth PA, Zhao Y, Fenton AM, Minnier J, Reddy AP, Klimek J, Yang X, David LL & Pamir N. Extended multiplexing of tandem mass tags (TMT) labeling reveals age and high fat diet specific proteome changes in mouse epididymal adipose tissue. *Molecular and Cellular Proteomics* 2017 **16** 873–890. (https://doi.org/10.1074/mcp.M116.065524)

24 Abbott KL, Nyre ET, Abrahante J, Ho YY, Isaksson Vogel R & Starr TK. The Candidate Cancer Gene Database: a database of cancer driver genes from forward genetic screens in mice. *Nucleic Acids Research* 2015 **43** D844–D848. (https://doi.org/10.1093/nar/gku770)

25 Tate JG, Bamford S, Jubb HC, Sondka Z, Beare DM, Bindal N, Boutselakis H, Cole CG, Creatore C, Dawson E, *et al.* COSMIC: the catalogue of somatic mutations in cancer. *Nucleic Acids Research* 2019 **47** D941–D947. (https://doi.org/10.1093/nar/gky1015)

26 Rahbari R, Zhang L & Kebebew E. Thyroid cancer gender disparity. *Future Oncology* 2010 **6** 1771–1779. (https://doi.org/10.2217/fon.10.127)

27 Dean DS & Gharib H. Epidemiology of thyroid nodules. *Best Practice and Research. Clinical Endocrinology and Metabolism* 2008 **22** 901–911. (https://doi.org/10.1016/j.beem.2008.09.019)

28 Lee ML, Chen GG, Vlantis AC, Tse GM, Leung BC & Van Hasselt CA. Induction of thyroid papillary carcinoma cell proliferation by estrogen is associated with an altered expression of Bcl-xL. *Cancer Journal* 2005 **11** 113–121. (https://doi.org/10.1097/00130404-200503000-00006)

29 Kim ES, Lim DJ, Baek KH, Lee JM, Kim MK, Kwon HS, Song KH, Kang MI, Cha BY, Lee KW, *et al.* Thyroglobulin antibody is associated with increased cancer risk in thyroid nodules. *Thyroid* 2010 **20** 885–891. (https://doi.org/10.1089/thy.2009.0384)

30 Nakamura S, Sakata S, Minamori Y, Komaki T, Kojima N, Kamikubo K, Yasuda K & Miura K. Serum thyroglobulin (Tg) concentration in healthy subjects absence of age-and sex-related differences. *Endocrinologia Japonica* 1984 **31** 93–98. (https://doi.org/10.1507/endocrj1954.31.93)

31 Liu WL, Cao YM, Liao T, Qu N, Zhu YX & Wei WJ. Multiple lectin assays in detecting glycol-alteration status of serum NRG1 in papillary thyroid cancer. *Translational Cancer Research* 2021 **10** 3218–3224. (https://doi.org/10.21037/tcr-20-1256)

32 He H, Li W, Liyanarachchi S, Wang Y, Yu L, Genutis LK, Maharry S, Phay JE, Shen R, Brock P, *et al.* The role of NRG1 in the predisposition to papillary thyroid carcinoma. *Journal of Clinical Endocrinology and Metabolism* 2018 **103** 1369–1379. (https://doi.org/10.1210/jc.2017-01798)

33 Chen F, Jin Y, Feng L, Zhang J, Tai J, Shi J, Yu Y, Lu J, Wang S & Li X. RRS1 gene expression involved in the progression of papillary thyroid carcinoma. *Cancer Cell International* 2018 **18** 1–12. (https://doi.org/10.1186/s12935-018-0519-x)

34 Fagerberg L, Hallström BM, Oksvold P, Kampf C, Djureinovic D, Odeberg J, Habuka M, Tahmasebpoor S, Danielsson A, Edlund K, *et al.* Analysis of the human tissue-specific expression by genome-wide integration of transcriptomics and antibody-based proteomics. *Molecular and Cellular Proteomics* 2014 **13** 397–406. (https://doi.org/10.1074/mcp.M113.035600)

35 Li N & Li S. RASAL2 promotes lung cancer metastasis through epithelial–mesenchymal transition. *Biochemical and Biophysical Research Communications* 2014 **455** 358–362. (https://doi.org/10.1016/j.bbrc.2014.11.020)

36 Feng M, Bao Y, Li Z, Li J, Gong M, Lam S, Wang J, Marzese DM, Donovan N, Tan EY, *et al.* RASAL2 activates RAC1 to promote triple-negative breast cancer progression. *Journal of Clinical Investigation* 2014 **124** 5291–5304. (https://doi.org/10.1172/JCI76711)

37 Im JY, Yoon SH, Kim BK, Ban HS, Won KJ, Chung KS, Jung KE & Won M. DNA damage induced apoptosis suppressor (DDIAS) is upregulated via ERK5/MEF2B signaling and promotes β-catenin-mediated invasion. *Biochimica et Biophysica Acta* 2016 **1859** 1449–1458. (https://doi.org/10.1016/j.bbagrm.2016.07.003)

38 Feng L, Wang R, Yang Y, Shen X, Shi Q, Lian M, Ma H & Fang J. KPNA4 regulated by miR-548b-3p promotes the malignant phenotypes of papillary thyroid cancer. *Life Sciences* 2021 **265** 118743. (https://doi.org/10.1016/j.lfs.2020.118743)

39 Mon SY, Riedlinger G, Abbott CE, Seethala R, Ohori NP, Nikiforova MN, Nikiforov YE & Hodak SP. Cancer risk and clinicopathological characteristics of thyroid nodules harboring thyroid-stimulating hormone receptor gene mutations. *Diagnostic Cytopathology* 2018 **46** 369–377. (https://doi.org/10.1002/dc.23915)

40 Hanahan D & Weinberg RA. The hallmarks of cancer. *Cell* 2000 **100** 57–70. (https://doi.org/10.1016/s0092-8674(00)81683-9)

41 Harsha HC & Pandey A. Phosphoproteomics in cancer. *Molecular Oncology* 2010 **4** 482–495. (https://doi.org/10.1016/j.molonc.2010.09.004)

42 Neumann S, Krohn K, Chey S & Paschke R. Mutations in the mouse TSH receptor equivalent to human constitutively activating TSH receptor mutations also cause constitutive activity. *Hormone and Metabolic Research* 2001 **33** 263–269. (https://doi.org/10.1055/s-2001-15119)

43 Ribeiro-Neto F, Urbani J, Lemee N, Lou L & Altschuler DL. On the mitogenic properties of Rap1b: cAMP-induced G1/S entry requires activated and phosphorylated Rap1b. *PNAS* 2002 **99** 5418–5423. (https://doi.org/10.1073/pnas.082122499)

44 Tsygankova OM, Saavedra A, Rebhun JF, Quilliam LA & Meinkoth JL. Coordinated regulation of Rap1 and thyroid differentiation by cyclic AMP and protein kinase A. *Molecular and Cellular Biology* 2001 **21** 1921–1929. (https://doi.org/10.1128/MCB.21.6.1921-1929.2001)

45 Shen CH, Yuan P, Perez-Lorenzo R, Zhang Y, Lee SX, Ou Y, Asara JM, Cantley LC & Zheng B. Phosphorylation of BRAF by AMPK impairs BRAF-KSR1 association and cell proliferation. *Molecular Cell* 2013 **52** 161–172. (https://doi.org/10.1016/j.molcel.2013.08.044)

46 Martin M & Marais R. Braking BRAF: AMPK leaves ERK stranded in the desert. *Molecular Cell* 2013 **52** 155–156. (https://doi.org/10.1016/j.molcel.2013.10.011)

47 Nelson ME, Parker BL, Burchfield JG, Hoffman NJ, Needham EJ, Cooke KC, Naim T, Sylow L, Ling NX, Francis D, *et al.* Phosphoproteomics reveals conserved exercise-stimulated signaling and AMPK regulation of store-operated calcium entry. *EMBO Journal* 2019 **38** e102578. (https://doi.org/10.15252/embj.2019102578)

48 López M, Varela L, Vázquez MJ, Rodríguez-Cuenca S, González CR, Velagapudi VR, Morgan DA, Schoenmakers E, Agassandian K, Lage R, *et al.* Hypothalamic AMPK and fatty acid metabolism mediate thyroid regulation of energy balance. *Nature Medicine* 2010 **16** 1001–1008. (https://doi.org/10.1038/nm.2207)

49 Hardie DG. Hot stuff: thyroid hormones and AMPK. *Cell Research* 2010 **20** 1282–1284. (https://doi.org/10.1038/cr.2010.153)

50 Wang T, Xu J, Bo T, Zhou X, Jiang X, Gao L & Zhao J. Decreased fasting blood glucose is associated with impaired hepatic glucose production in thyroid-stimulating hormone receptor knockout mice. *Endocrine Journal* 2013 **60** 941–950. (https://doi.org/10.1507/endocrj.ej12-0462)

51 Andrade BM, Araujo RL, Perry RL, Souza EC, Cazarin JM, Carvalho DP & Ceddia RB. A novel role for AMP-kinase in the regulation of the Na+/I−-symporter and iodide uptake in the rat thyroid gland. *American Journal of Physiology-Cell Physiology* 2011 **300** C1291–C1297. (https://doi.org/10.1152/ajpcell.00136.2010)

52 Liu S, Jing F, Yu C, Gao L, Qin Y & Zhao J. AICAR-induced activation of AMPK inhibits TSH/SREBP-2/HMGCR pathway in liver. *PLoS One* 2015 **10** e0124951. (https://doi.org/10.1371/journal.pone.0124951)

53 Aw DKL, Sinha RA, Xie SY & Yen PM. Differential AMPK phosphorylation by glucagon and metformin regulates insulin signaling in human hepatic cells. *Biochemical and Biophysical Research Communications* 2014 **447** 569–573. (https://doi.org/10.1016/j.bbrc.2014.04.031)

54 Bossis I & Stratakis CA. Minireview: PRKAR1A: normal and abnormal functions. *Endocrinology* 2004 **145** 5452–5458. (https://doi.org/10.1210/en.2004-0900)

55 Wang Y-T, Tsai C-F, Hong T-C, Tsou C-C, Lin P-Y, Pan S-H, Hong T-M, Yang P-C, Sung T-Y & Hsu W-L. An informatics-assisted label-free quantitation strategy that depicts phosphoproteomic profiles in lung cancer cell invasion. *Journal of Proteome Research* **2010** 5582–5597. (https://doi.org/10.1021/pr100394u)

56 Kirschner LS, Carney JA, Pack SD, Taymans SE, Giatzakis C, Cho YS, Cho-Chung YS & Stratakis CA. Mutations of the gene encoding the protein kinase A type I-α regulatory subunit in patients with the Carney complex. *Nature Genetics* 2000 **26** 89–92. (https://doi.org/10.1038/79238)

57 Correa R, Salpea P & Stratakis CA. Carney complex: an update. *European Journal of Endocrinology* 2015 **173** M85–M97. (https://doi.org/10.1530/EJE-15-0209)

58 Ledent C, Denef JF, Cottecchia S, Lefkowitz R, Dumont J, Vassart G & Parmentier M. Costimulation of adenylyl cyclase and phospholipase C by a mutant alpha 1B-adrenergic receptor transgene promotes malignant transformation of thyroid follicular cells. *Endocrinology* 1997 **138** 369–378. (https://doi.org/10.1210/endo.138.1.4861)

59 He H, Li W, Liyanarachchi S, Jendrzejewski J, Srinivas M, Davuluri RV, Nagy R & De La Chapelle A. Genetic predisposition to papillary thyroid carcinoma: involvement of FOXE1, TSHR, and a novel lincRNA gene, PTCSC2. *Journal of Clinical Endocrinology and Metabolism* 2015 **100** E164–E172. (https://doi.org/10.1210/jc.2014-2147)

60 Haymart MR, Repplinger DJ, Leverson GE, Elson DF, Sippel RS, Jaume JC & Chen H. Higher serum thyroid stimulating hormone level in thyroid nodule patients is associated with greater risks of differentiated thyroid cancer and advanced tumor stage. *Journal of Clinical Endocrinology and Metabolism* 2008 **93** 809–814. (https://doi.org/10.1210/jc.2007-2215)

61 Boelaert K. The association between serum TSH concentration and thyroid cancer. *Endocrine-Related Cancer* 2009 **16** 1065–1072. (https://doi.org/10.1677/ERC-09-0150)

62 Franco AT, Malaguarnera R, Refetoff S, Liao XH, Lundsmith E, Kimura S, Pritchard C, Marais R, Davies TF, Weinstein LS, *et al.* Thyrotrophin receptor signaling dependence of Braf-induced thyroid tumor initiation in mice. *PNAS* 2011 **108** 1615–1620. (https://doi.org/10.1073/pnas.1015557108)

63 Knauf JA, Ma X, Smith EP, Zhang L, Mitsutake N, Liao XH, Refetoff S, Nikiforov YE & Fagin JA. Targeted expression of BRAFV600E in thyroid cells of transgenic mice results in papillary thyroid cancers that undergo dedifferentiation. *Cancer Research* 2005 **65** 4238–4245. (https://doi.org/10.1158/0008-5472.CAN-05-0047)

64 Lu C, Zhao L, Ying H, Willingham MC & Cheng SY. Growth activation alone is not sufficient to cause metastatic thyroid cancer in a mouse model of follicular thyroid carcinoma. *Endocrinology* 2010 **151** 1929–1939. (https://doi.org/10.1210/en.2009-1017)

Received 11 March 2023
Accepted 30 August 2023
Available online 1 September 2023
Version of Record published 3 October 2023